FTIR Spectroscopy of NH_3 on Acidic and Ionotropic Alginate Aerogels

Romain Valentin,[†] Raluca Horga,[†] Barbara Bonelli,[‡] Edoardo Garrone,[‡] Francesco Di Renzo,[†] and Françoise Quignard*[,†]

Laboratoire de Matériaux Catalytiques et Catalyse en Chimie Organique, UMR 5618 CNRS-ENSCM-UM1, Institut C. Gerhardt, FR 1878, 8 rue de l'Ecole Normale, 34296 Montpellier Cedex 5, France, and Dipartimento di Scienza dei Materiali e Ingegneria Chimica, Politecnico di Torino, Corso Duca degli Abruzzi 24, 10129 Torino, Italy

Received August 6, 2005; Revised Manuscript Received December 17, 2005

The acidity of alginate aerogel films has been investigated by infrared spectroscopy of adsorbed NH_3. Supercritical drying of the alginate provided samples with a surface area of several hundred square meters per gram, in which the probe molecule could reach all acidic sites. Free carboxylic groups were studied on acid-gelled alginates and were found to behave as effective Brønsted acid sites. Ionotropic alginate gels formed by alkaline earth cations presented only the Lewis acidity of the cations. Ionotropic gels formed by transition metal cations presented both Lewis and Brønsted sites, because of the presence of a fraction of free carboxylic groups. The incomplete salification was correlated to the pH of the gelling solutions.

Introduction

Alginates are natural polysaccharides produced by brown algae.[1] Their block copolymer chain is composed of (1−4)-linked uronate residues (pyranose rings with a carboxylic group in C-6; Figure 1). β-D-Mannuronate and α-L-guluronate residues are present in varying proportions, sequences, and molecular weights.[2−4] The different orientations of the (1−4)-links of the mannuronate residues, axial in the case of guluronate and equatorial in the case of mannuronate, account for variations of the organization and stability of the gels formed by alginates with different mannuronic/guluronic (M/G) ratios.

Most applications of alginates in drug-release systems[5] and as supports in biocatalysis are based on their ability to form strong heat-stable gels with divalent or trivalent cations. Monovalent metal ions form soluble salts with alginate, whereas divalent or multivalent cations, except Mg^{2+}, form gels. Cations show different affinities for alginate, and selective ion binding is the basis for the ability of alginate to form ionotropic hydrogels. The interaction of the polyuronate chains with various divalent cations has been monitored by circular dichroism (CD).[6−8] Differences in CD behavior with Mg^{2+}, Ca^{2+}, and Sr^{2+} are consistent with the greater selectivity of ion binding. Spectral changes when gelation is induced by Cu^{2+} suggest a less specific binding mechanism, consistent with the lack of selectivity of Cu^{2+} for different polyuronates.[9]

Calorimetric and dilatometric methods have shown that the nature of the divalent cations has a great influence on the network elasticity.[10,11] The Young modulus of the gels follows the order Cd > Ba > Cu > Ca > Ni > Co > Mn. Alginates with high guluronic content give gels with a higher strength than alginates with low guluronic content. This difference can be attributed to the stronger affinity of the guluronic residues for divalent cations.[12−14] The effects of metal ion complexation on the morphology of the resultant gels were evaluated by polarized optical microscopy and electron microscopy.[15−17]

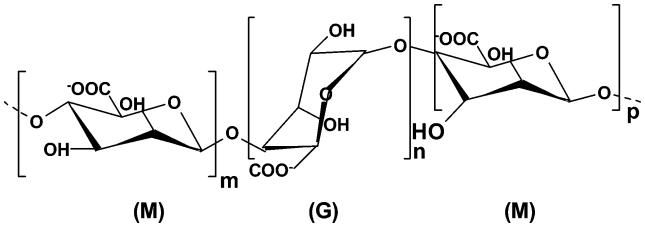

Figure 1. Structural units of alginate. M, mannuronate residue; G, guluronate residue.

A less frequently cited method for forming an alginate gel is to lower the pH of a sodium alginate solution. The alginic acid gels formed in this way have been known and used for a long time,[5,18] but the understanding of these gels is poor, as compared to the more extensively studied ionotropic gels. The effects of chemical composition and molecular weight on gel strength and gelling kinetics have been studied.[12] Acidic gels, similarly to ionotropic gels, present a higher mechanical strength for a high guluronic content. Small-angle X-ray scattering (SAXS) suggests the formation of junction zones with a high degree of multiplicity.[19,20] The amorphous state of the gelified alginates prevents more detailed structural information from being obtained by X-ray crystallography.

The earliest infrared spectroscopy studies of alginates were parts of more extensive works directed at the identification of different polysaccharides through the vibrational frequencies of their functional groups.[21] Calculation of the IR vibrational frequencies allowed the assignment of most observed bands.[22,23] Infrared methods have been proposed for the estimation of the mannuronic/guluronic ratio.[24−27] The values obtained by infrared spectroscopy were in very good agreement with the results of more cumbersome destructive procedures. Very few studies have addressed the ion-exchange process between Na^+ and M^{2+}. Sartori et al.[28] quantitatively correlated the peak wavenumbers of FTIR spectra to the Na^+ and Ca^{2+} content.

* To whom correspondence should be addressed. Fax: + 33 467163470. Tel.: + 33 467163460. E-mail: quignard@enscm.fr.

[†] Institut C. Gerhardt.

[‡] Politecnico di Torino.

10.1021/bm050559x CCC: $33.50
Published on Web 02/08/2006

Although these works provided a sound vibrational characterization of the alginate gels, the preparation of the samples prevented any spectroscopic study of the reactivity of the functional groups. FTIR spectroscopy of adsorbed probe molecules is a powerful method for investigating the states of cations and acidic groups, as witnessed by the widespread application of this technique in the study of inorganic solids or, less frequently, high-surface-area polymers.[29−32] However, the wafers of dried polysaccharides used for spectroscopic studies in the past presented very small surface areas. As a result, an insufficient fraction of functional groups was accessible for a significant study of their interactions with probe molecules.

The aim of the present article is to demonstrate the unique possibilities offered by supercritical drying to prepare alginate samples in which a large fraction of uronic groups is accessible. In CO_2 supercritical extraction, the shrinkage induced by capillary evaporation is prevented, and the solid prepared in this way, known as an aerogel, retains a high degree of dispersion. Indeed, alginate aerogel microspheres can present very high surface areas, close to 300 $m^2\ g^{-1}$.[33] The surface functional groups of the polysaccharide are thus accessible to probe molecules.[34]

In this work, the FTIR spectroscopy of adsorbed NH_3 has been used to investigate the acidity of alginate aerogel films prepared in the presence of different cations. Ammonia was chosen as the probe because of its ability to differentiate between Lewis and Brønsted acid sites and because of its small size, similar to the size of the water molecule.[35,36]

Materials and Methods

Preparation of the Alginate Gels. Polysaccharide hydrogels were prepared using two methods of gelation, based on exchange with divalent cations or on the lowering of pH.

Ionotropic Gelation. A 1% (w/w) solution of sodium alginate (Sigma-Aldrich from *Macrocystis pyrifera*, 3600 cP viscosity of a 2% solution, mannuronic/guluronic ratio of 1.82 by spectroscopic evaluation[24]) in deionized water was spread out at room temperature in a Petri dish and gently covered by a 0.24 M solution of $M(NO_3)_2$ (5 times the volume of the alginate solution). Nitrates of Ba, Ni, Co, and Cu from Aldrich were used. The film was cured in the gelation solution for 22 h.

Acidic Gelation. A 2% (w/w) solution of sodium alginate (10 cm^3) was cooled to 275 K. Ground maleic anhydride (0.2 g) was dispersed in the polymer solution and left to hydrolyze until a hydrogel monolith was obtained.[37] The monolith was washed with water and dried. After supercritical drying, aerogel wafers were cut from the monolith.

Because of the difficulty of cutting monolith xerogels to the appropriate thickness for IR spectroscopy, acidic xerogels were prepared by a different procedure: A 1% sodium alginate solution was spread out at room temperature in a Petri dish and covered by 5 times the volume of HCl solution (0.5 M). The film was cured in the gelation solution for 2 h and washed with water until pH 7 was reached.

Hydrogel Drying. Xerogel films were obtained after drying of the hydrogels on glass plates in an oven at 50 °C. To obtain the aerogel films, intermediate alcogels were formed by immersion of the hydrogel films in a series of successive ethanol/water baths of increasing alcohol concentration (10, 30, 50, 70, 90, and 100%) for 15 min each.[38] The aerogel films were obtained by drying the alcogels under supercritical CO_2 conditions (74 bar, 31.5 °C) in a Polaron 3100 apparatus. In this article, samples with different M^{2+} cations are labeled M-alg aerogel or M-alg xerogel according to the drying process. Cation contents were determined by ICP and are reported in Table 1. Also reported in Table 1 are the amounts of moisture adsorbed by the aerogels upon storage, which could be easily desorbed by heating under vacuum at 323 K.

Table 1. Cation and Water Contents, Surface Areas, and Densities of the Aerogel and Xerogel Samples

sample	M^{2+} (wt %)	Na^+ (wt %)	mass loss upon outgassing at 323 K (%)	S_{BET} ($m^2\ g^{-1}$)	porosity
Ba-alg aerogel	22.0	0.015	15.8	301 ± 6	0.985 ± 0.005
Co-alg aerogel	10.5	0.007	22.4	298 ± 6	0.978 ± 0.003
Ni-alg aerogel	12.0	0.07	11.6	187 ± 4	0.986 ± 0.002
Cu-alg aerogel	12.0	0.006	15.2	356 ± 7	0.982 ± 0.003
H-alg aerogel	−	<0.005	11.0	391 ± 8	0.83 ± 0.05
H-alg xerogel	−	<0.005	8.2	1.3 ± 0.5	0.1 ± 0.3

Measurement of Textural Properties. Nitrogen adsorption/desorption isotherms were recorded in a Micromeritics ASAP 2010 apparatus at 77 K after the sample had been outgassed at 323 K under vacuum until a stable 3×10^{-5} mbar pressure was obtained without pumping. The aerogel surface areas evaluated by the BET method are reported in Table 1 and cover the range 180−400 $m^2\ g^{-1}$. The corresponding xerogels presented surface areas lower than 2 $m^2\ g^{-1}$. The high dispersion of the aerogels is confirmed by the porosity (ratio between the volume of the polysaccharide and the volume of the gel) data reported in Table 1. The porosity data were obtained by the mass/volume ratio of microspheres prepared from the same batches of solution from which the films were prepared.[33,39] In the case of the ionotropic aerogels, the porosity was generally higher than 98%. The acidic aerogel was slightly denser, whereas it was dubious whether the xerogel presented any porosity, the calculated value being smaller than the standard error due to the measurement of the gel volume.

Infrared Spectroscopy. Suitable wafers were cut from the alginate films and placed into a homemade all-silica cell provided with KBr windows for transmission IR measurements. The wafers were supported by a gold case. The cell also allows evacuation, heat treatment, and gas dosage. FTIR spectra were recorded on a Bruker Vector 22 spectrometer equipped with a DTGS detector. Adsorption of ammonia was carried out on wafers evacuated in situ at 323 K (residual pressure $<10^{-6}$ mbar). In all cases, the equilibrium was attained in a few minutes, and no evidence was observed of any slow diffusional processes, even with the xerogel.

Results

Acidic Alginate Films. Infrared spectra of both xerogel and aerogel wafers of H-alginate, the gel formed by pH lowering in the absence of divalent cations, are reported in Figure 2 (spectrum a for the xerogel and d for the aerogel). Both spectra present bands at the same wavenumbers: a broad band due to O−H stretching modes with a maximum around 3460 cm^{-1}, C−H stretching bands in the 2960−2840 cm^{-1} range, C−O stretching modes of the carboxyl group between 1750 and 1400 cm^{-1}, a region of bending modes between 1500 and 1200 cm^{-1}, and a region of C−O and C−C stretching modes between 1200 and 1000 cm^{-1}.[22,40]

The most intense band related to the acidic functional group is the C═O stretching mode of the free carboxyl group at 1735 cm^{-1}. A weak band, attributed to the antisymmetric mode of the carboxylate group, is observed at 1577 cm^{-1} for the xerogel (spectrum a) and 1593 cm^{-1} in the aerogel (spectrum d). Its presence suggests that a small fraction of the carboxylic groups are deprotonated in the virtual absence of any mineral cation (Table 1). A band at 3350 cm^{-1} observable for the xerogel can be attributed to the O−H stretching mode of water in clusters interacting with a proton.[31] Two weak broad bands at 2620 and

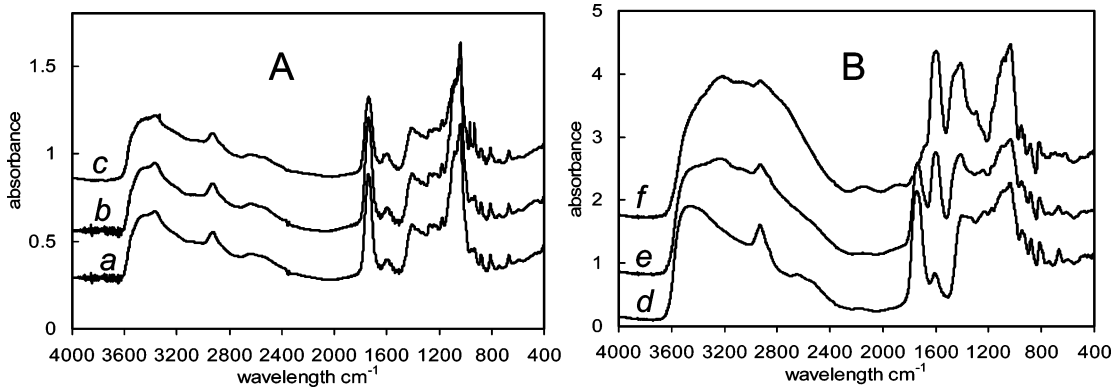

Figure 2. Adsorption of NH_3 on (A) H-alg xerogel and (B) H-alg aerogel. NH_3 pressure: (a,d) 0, (b,e) 1, (c) 38, and (f) 33 mbar. Spectra a, c, d, and f are offset by −0.3, 0.3, −0.8, and 0.8 absorbance units, respectively.

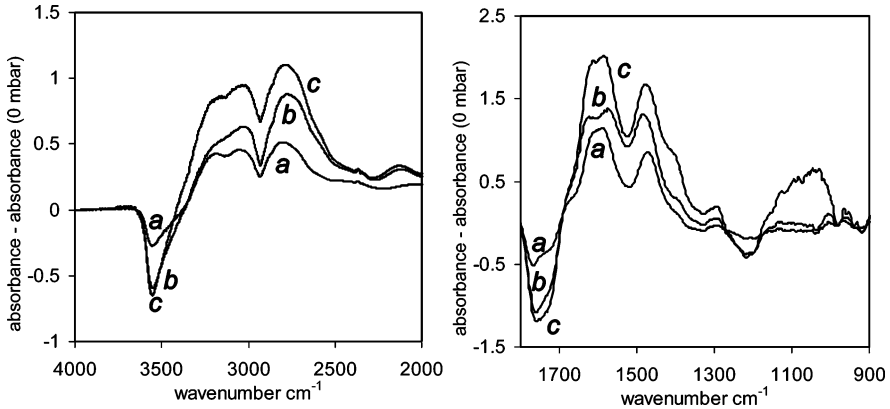

Figure 3. Difference spectra of adsorption of NH_3 on H-alg aerogel. NH_3 pressure: (a) 1, (b) 6, and (c) 33 mbar.

2510 cm^{-1} are classically observed in the case of dimeric acids and correspond to the head-to-head interaction of two COOH groups.

The spectra of the xerogel after adsorption of ammonia are reported in Figure 2 (spectra b and c) and do not significantly differ from the spectrum before ammonia adsorption (Figure 2a). The two "horns" of gaseous ammonia at 966 and 932 cm^{-1} are clearly present in the spectrum at equilibrium with 38 mbar NH_3.

Adsorption of ammonia on the H-alginate aerogel led to significant changes in the IR spectra (spectra e and f), which correspond to the transfer of a proton from a carboxyl group to an ammonia molecule. Ammonia salifies the carboxyl group, with the formation of a carboxylate $COO^-NH_4^+$. Detailed information is provided by the difference spectra reported in Figure 3, in which the absorbance of the aerogel before adsorption is subtracted, wavelength by wavelength, from the absorbance after adsorption of ammonia.

At increasing NH_3 pressure, a negative difference band develops at 3545 cm^{-1}, corresponding to the disappearance of the O−H stretching mode of free carboxyl groups. The three curves cross each other in a common range around 3360 cm^{-1}. Taking into account a possible variation of the transparency of the wafer with adsorption, this can be considered as evidence that an isosbestic point is present at 3360 cm^{-1}. This suggests that the positive band envelope extending from this wavelength onward is due to the reaction products, i.e., ammonium species interacting with the surroundings and in particular H-bonded to the carboxylate groups. This band envelope shows a complex structure, with maxima at 3180, 3020, and 2770 cm^{-1}. Absorption between 3050 and 2650 cm^{-1} should be due to the N−H stretching of NH_4^+.[41] The maximum at 3180 cm^{-1} could be attributed to an overtone band of the antisymmetric C−O stretching of carboxylate species at 1600 cm^{-1}. The band envelope of adsorbed ammonium species is interrupted by gaps at 2922 and 2858 cm^{-1}, which appear as negative bands superimposed on a more intense positive absorption at frequencies that correspond to the C−H stretching bands. This suggests an uncommon perturbation of the C−H groups by ammonia adsorption.

The broad bands of the dimeric acid observed at 2630 and 2510 cm^{-1} in the spectrum of the aerogel (Figure 2, spectrum d) disappear with ammonia adsorption (Figure 2, spectra e and f), as the acid groups are salified.

Negative difference bands at 1760 and 1725 cm^{-1} develop with ammonia adsorption (Figure 3), corresponding to the disappearance of the C−O stretching of the free acid groups (1735 cm^{-1}, Figure 2B). Beyond an isosbestic point at 1695 cm^{-1}, positive difference bands at 1620 and 1575 cm^{-1} correspond to the asymmetric C−O stretching of two types of carboxylate species. A difference band at 1470 cm^{-1} appears and grows with ammonia pressure and corresponds to the N−H bending of adsorbed NH_4^+.[41] A minor positive band at 1400 cm^{-1} can be attributed to the symmetric C−O stretching of carboxylate species.

A negative difference band around 1215 cm^{-1} appears with ammonia adsorption, corresponding to the disappearance of a band at 1230 cm^{-1} in the H-alg aerogel (Figure 2, spectrum d). This band is not present in salified alginates, as shown later, and is typical of free carboxylic acids.[40] A corresponding isosbestic point is observed at 1180 cm^{-1}.

Ionotropic Alginate Films. The FTIR spectra of the aerogels obtained from ionotropic gelation with several divalent cations are reported in Figure 4. The spectrum of the Ba-alg aerogel differs from the spectrum of the H-alg aerogel (Figure 2d) by the absence of several bands related to the free acid group. The

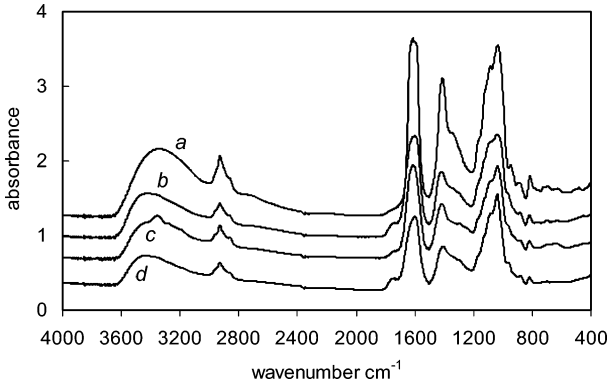

Figure 4. FTIR spectra of ionotropic alginate aerogels: (a) Ba-alg, (b) Co-alg, (c) Ni-alg, and (d) Cu-alg. Spectra offset for clarity.

maximum of the O−H stretching band for the Ba-alg aerogel is at 3320 cm^{-1}, at a significantly lower wavenumber than the corresponding band at 3460 cm^{-1} for H-alg. The bands of the dimeric acid at 2620 and 2510 cm^{-1} are absent for the Ba-alg aerogel, as is the band of asymmetric C−O stretching of COOH at 1735 cm^{-1}. The most intense band of the spectrum is the asymmetric stretching of the carboxylate group at 1605 cm^{-1}. No band is observed at 1200 cm^{-1}, where the C−O bending of the free carboxylic group is expected.

The spectra of ionotropic aerogels formed in the presence of transition metal cations differ to some extent from the spectrum of the Ba-alg aerogel and indicate the presence of some residual free COOH groups (Figure 4). The maximum of the O−H stretching band is at 3420 cm^{-1}, a wavenumber nearer to the value for H-alg than for Ba-alg aerogel. For all transition metal cation aerogels, a band of the asymmetric C−O stretching of the free acid group is observed at 1740 cm^{-1}. The free acid band is much weaker than the band of carboxylate at 1600 cm^{-1}.

A band at 3335 cm^{-1} is observed for the Ni-alg aerogel. This band, corresponding to the O−H stretching of a water cluster around a proton, has to be related to the band observed at 3350 cm^{-1} for the H-alg xerogel. Retention of water is normal in a conventionally dried xerogel, but it is an indication of faulty dehydration in the case of a supercritically dried aerogel. Indeed, partial dehydration can account for the lower surface area of the Ni-alg aerogel sample compared to the surface areas of the other aerogels (Table 1).

The effects of adsorption of NH_3 on ionotropic aerogels are lower than in the case of adsorption on acidic aerogel, and they can be more easily observed in difference spectra. The difference spectra of ammonia adsorption on the Ba-alg aerogel wafers are reported in Figure 5. They do not present any well-defined negative bands, as were observed in the case of the H-alg aerogel. This indicates that the adsorption of the probe molecule does not perturb the frequency of the vibrators of the adsorbent. Upon adsorption of ammonia, difference bands appear at 3370 and 3225 cm^{-1}, typical of molecularly adsorbed NH_3.[41] The increase of absorbance at 1605 cm^{-1} can also be attributed to adsorbed NH_3. The formation of these bands indicates that NH_3 is adsorbed on Lewis acid sites, namely, the metal cations present in the system. The adsorption of ammonia increases the overall polarity of the system, as indicated by the increased absorbance of several bands not related to the N−H vibrations, such as the C−H stretching bands between 2945 and 2845 cm^{-1}; the asymmetric and symmetric C−O stretching modes of carboxylate at 1605 and 1410 cm^{-1}, respectively; and the bands at 1165, 1116, and 1085 cm^{-1}.

The difference spectra of ammonia adsorption on a film of Ni-alg aerogel, a representative transition metal cation ionotropic gel, are reported in Figure 6. A negative difference band at 3545 cm^{-1} corresponds to the disappearance of the O−H stretching of the free COOH groups, due to the transfer of their proton and the formation of ammonium cations. However, most ammonia is molecularly adsorbed without proton transfer, as indicated by the strong bands at 3345 cm^{-1} and in the 3265−3180 cm^{-1} range. The absorbance of the C−H stretching bands in the 2950−2850 cm^{-1} range increases, as in the case of Ba-alg aerogel.

The negative difference bands at 1745 and 1675 cm^{-1} confirm the disappearance of the free acid groups, and the band at 1480 cm^{-1} can be attributed to hydrogen-bonded NH_4^+. The other bands of the spectrum can be interpreted as in the case of the molecular adsorption of NH_3 on the Ba-alg aerogel.

Discussion

Aerogel−Xerogel Comparison. The preparation of a stable aerogel is a prerequisite to the study of the interactions between polysaccharides and reactive gases. The ammonia adsorptions on aerogels and xerogels differ dramatically, as evidenced in Figure 2 in the case of acid-gelled alginate. Equilibration with more than 30 mbar of NH_3 does not allow any measurable interaction between the probe molecule and the xerogel to be observed, whereas an equivalent pressure of NH_3 brings about the salification of all of the acidic sites of the aerogel.

The different accessibilities of the acidic functions in xerogels and aerogels can be partially justified by their different surface areas. The surface areas of the alginate aerogels are more than 100 times larger than the surface areas of the corresponding xerogels (Table 1). This difference is the result of the different aggregation states of the fibrils that form the gel. In the case of the aerogels, the fibrils are quite far apart and present a limited number of contact points, as in the parent hydrogel. In the case of the xerogels, the capillary tension of the water−vapor interface drives the hydrogel fibrils together and forms a compact solid.

The high surface areas of the aerogels do not imply that all acidic functions are situated at the surface of the gel fibrils. It has been shown that the surface area of an alginate aerogels can be correlated to the size of the aggregates of macromolecules.[33] In the case of cylindrical fibrils, a surface area of 391 $m^2\ g^{-1}$, as in the case of the H-alg aerogel, would correspond to a fibril diameter of 15.3 nm. In such a configuration, a large fraction of the acidic chains are not located at the fibril surface. However, they are accessible to ammonia molecules, which can penetrate inside the fibrils of the aerogel much more easily than in the 10000-times thicker film of the xerogel.

Ammonia interacts with alginate aerogel according to two distinct mechanisms: molecular adsorption on electron-acceptor sites (Lewis acid) or proton transfer from a Brønsted acid site and electrostatic bonding of the resulting ammonium cation to an anionic site of the adsorbent.

In the adsorption of ammonia on the H-alg aerogel, the bands of the free carboxylic acid disappear and are replaced by the bands of carboxylate, whereas the bands of adsorbed ammonium appear. This demonstrates that the carboxylic acids of the alginate are effective Brønsted sites. Such easy proton transfer can contribute to an old debate on the adsorption of ammonia on acid sites. Proton transfer was considered to be easier from acid sites at a solid surface than from gas-phase acid molecules.[42] This effect was diversely attributed to the stabilization of the ammonium ion inside a porous system[35] or to experimental problems in the gas phase, such as acid dimerization or precipitation of the salified acid.[43]

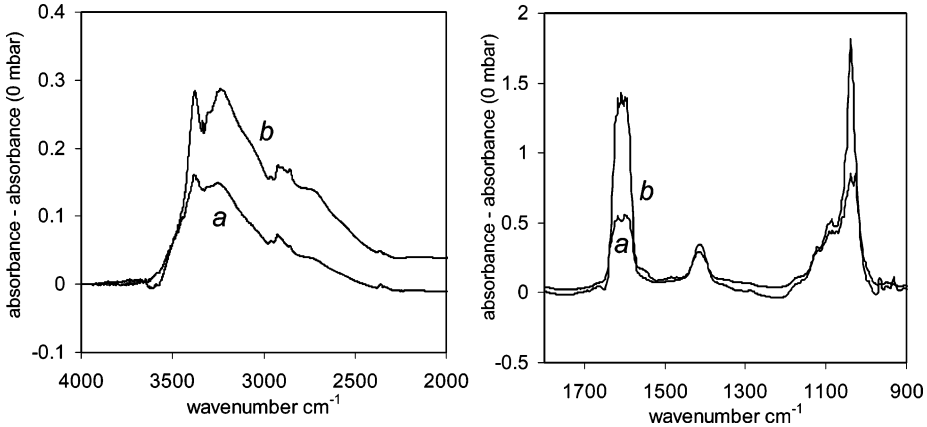

Figure 5. Difference spectra of NH_3 adsorption on Ba-alg aerogel. NH_3 pressure: (a) 1 and (b) 28 mbar.

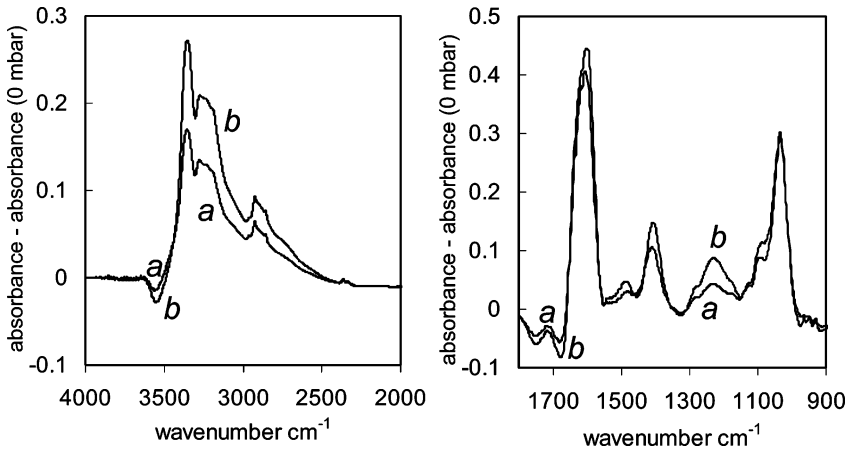

Figure 6. Difference spectra of NH_3 adsorption on Ni-alg-aero. NH_3 pressure: (a) 1 and (b) 6 mbar.

The very intense band at 1735 cm^{-1} indicates that, in the outgassed H-alg aerogel, most acid sites are free from hydrogen bonding. Head-to-head acid dimers are present, and they separate when the ammonium salts are formed. This could not occur without a significant change of the geometry of adjacent polymer chains. The influence of the adsorbed molecules on the aggregation of the chains is the basis for the evolution from the hydrogel to the supercritically dried aerogel or the conventionally dried xerogel. It is important to determine the point at which the structure of the hydrogel is retained after drying. It has been shown that the linear shrinkage during the supercritical drying of alginate hydrogels can be lower than 10%.[33] Such a preservation of the gel volume suggests that the aerogel retains the main parameters of the structure of the hydrogel, such as the aggregation number of the chains and the overall shape of the fibrils. However, the finer interactions between polymer chains are expected to be modified by dehydration, alcohol exchange, and CO_2 extraction, as they are modified by ammonia adsorption.

Competition between Acidic and Ionotropic Gelling. Spectroscopic evidence shows that, in the Ba-alg aerogel, an alginate gel formed by alkaline earth cations, all carboxylic groups are salified. In this case, no proton-exchange sites are available, and the adsorption of ammonia takes place through interactions with the available Lewis acids, namely, the barium cations. The divalent cations already interact with the four oxygen atoms of two carboxylate groups, and the molecular adsorption of ammonia corresponds to an expansion of the coordination sphere of the cation.

Modifications of the environment of the adsorption site are expected to bring about a change of the overall polarity of the system, as well as some changes of the geometry of the chains. This can account for the variations of absorbance of vibrators not directly implicated in the ammonia adsorption, such as the C−H bonds of the carbohydrate ring. It is remarkable that the absorbance of the C−H vibrations increases upon adsorption of ammonium on the carboxylic acid and decreases upon molecular adsorption of ammonia on the divalent cations.

Table 2. pH of the Gelling Solution and Carboxylate/(Carboxylate + Carboxylic Acid) Ratio from the Intensities of the IR Bands of Carboxylic Acid (1735 cm^{-1}) and Carboxylate (1600 cm^{-1})

		salification ratio	
sample	gelling solution pH	outgassed sample	after NH_3 adsorption
Ba-alg aerogel	5.60	1.00	1.00
Co-alg aerogel	4.20	0.88	1.00
Ni-alg aerogel	3.94	0.93	1.00
Cu-alg aerogel	3.51	0.87	1.00
H-alg aerogel	1.94	0.20	0.85

In the case of the ionotropic gels formed by transition metal cations, a significant fraction of the carboxylic groups are not salified, as indicated by the ratios of the intensities of the antisymmetric stretching modes of carboxylic acid (1735 cm^{-1}) and carboxylate (1600 cm^{-1}) reported in Table 2. If the extinction coefficients of the two bands are assumed to be equivalent, the degree of salification of the carboxylic group corresponds to $I_{1600}/(I_{1600} + I_{1735})$ and decreases in the order Ba > Ni ≥ Co ≈ Cu ≫ H. In the case of the H-alg aerogel, residual water molecules can contribute to the 1600 cm^{-1} signal and cause an overestimation of the salification ratio.

The level of salification of the acid groups does not correspond to the scale of affinity of the alginate for divalent cations, which has been claimed to follow the order Cu > Ba > Ca > Ni > Zn > Co.[44] Indeed, this scale of affinity was determined by competitive exchange of a small amount of cations in the presence of a large amount of H,Na-alginate. Under gelling conditions, a large excess of divalent cation is present. As a consequence, the divalent cations can reach exchange equilibrium with the alginate, and the pH of the solution is controlled by the dissociation constants of the cation hydroxides, which decrease in the order Ba ≫ Ni ≈ Co ≥ Cu, in good agreement with the experimental pH of the system, reported in Table 2.

In gelling systems with a pH higher than the pK_a of the alginate (4.2),[45] as in the Ba-alg system, the acidic groups are completely salified, whereas in systems with a lower pH, as in the case of solutions of transition metal salts, a significant fraction of the acidic groups of the alginate remain in the hydrogen form. The logical implication is that, in the case of the transition metal systems, the gelling mechanism is intermediate between the ionotropic and acidic mechanisms. Ammonia adsorption takes place both on the divalent cation and by proton transfer from the available Brønsted sites.

Conclusions

The preparation of aerogels by alcohol exchange and CO_2 supercritical drying of alginate hydrogels allows the dispersion of the polysaccharide fibrils to be retained and makes them susceptible to being studied by spectroscopy of probe molecules adsorbed from the gas phase. In the case of alginate aerogels, infrared spectroscopy allows differentiation between ammonia adsorbed as such on the Lewis acid sites corresponding to the gelling cations and ammonia protonated by the carboxylic groups of the polysaccharide.

In the case of acidic gels, head-to-head dimers of the carboxylic groups are observed and probably make an important contribution to the mechanism of gelation. The salification of these groups by ammonium cations indicates that the probe molecules can penetrate inside the 15-nm fibrils of the aerogel.

The ratio between salified and free carboxyl groups is a useful tool for characterizing gels formed at pH levels at which ionotropic and acidic gelation mechanisms compete. It appears clear that acidic gelation can contribute to the formation of gels in the presence of transition metal cations if the pH is not otherwise controlled. The aerogels formed under these conditions present both the Lewis sites of the ionotropic gels and the Brønsted sites of the acidic gels.

Acknowledgment. The authors are grateful to the Région Languedoc-Roussillon for financial support.

References and Notes

(1) McHugh, D. J. *A Guide to the Seaweed Industry*; FAO: Rome, 2003; p 27.
(2) Barbotin, J. N.; Nava Saucedo, J. E. In *Polysaccharides*; Dumitriu, S., Ed.; Marcel Dekker: New York, 1998; p 749.
(3) Sime, W. J. In *Food Gels*; Harris, P., Ed.; Elsevier: Amsterdam, 1990; p 53.
(4) Chen, J. P.; Hong, L.; Wu, S.; Wang, L. *Langmuir* **2002**, *18*, 9413.
(5) Tønnesen, H. H.; Karlsen, J. *Drug Dev. Ind. Pharm.* **2002**, *28*, 621.
(6) Grant, G. T.; Morris, E. R.; Rees, D. A.; Smith, P. J. C. *FEBS Lett.* **1973**, *32*, 195.
(7) Morris, E. R.; Rees, D. A.; Thorn, D.; Boyd, J. *Carbohydr. Res.* **1978**, *66*, 145.
(8) Morris, E. R.; Rees, D. A.; Young, G. *Carbohydr. Res.* **1982**, *108*, 181.
(9) Thom, D. T.; Grant, G. T.; Morris, E. R.; Rees, D. A. *Carbohydr. Res.* **1982**, *100*, 29.
(10) Cesaro, A.; Delben, F.; Paoletti, S. *J. Chem. Soc., Faraday Trans. 1* **1988**, *84*, 2573.
(11) Ouwerx, C.; Velings, N.; Mestdagh, M. M.; Axelos, M. A. V. *Polym. Gels Networks* **1998**, *6*, 393.
(12) Draget, K. I.; Skjak-Braek, G.; Smidsrød, O. *Carbohydr. Polym.* **1994**, *25*, 31.
(13) Wang, X.; Spencer, H. G. *Polymer* **1998**, *39*, 2759.
(14) Siew, C. K.; Williams, P. A.; Young, N. W. G. *Biomacromolecules* **2005**, *6*, 963.
(15) Sterling, C. *Biochim. Biophys. Acta* **1957**, *26*, 186.
(16) Yokoyama, F.; Achife, E. C.; Matoka, J.; Shimamura, K.; Yamashita, Y.; Monobe, K. *Polymer* **1991**, *32*, 2911.
(17) Yokoyama, F.; Achife, E. C.; Takahira, K.; Yamashita, Y.; Monobe, K. *J. Macromol. Sci. Phys.* **1992**, *B31*, 463
(18) Mongar, I. L.; Wassermann, A. *J. Chem. Soc.* **1952**, 492.
(19) Draget, K. I. *Annu. Trans. Nordic Rheol. Soc.* **2001**, *8/9*, 149.
(20) Draget, K. I.; Stokke, B. T.; Yuguchi, Y.; Urakawa, H.; Kajiwara, K. *Biomacromolecules* **2003**, *4*, 1661.
(21) Aspinall, G. O., Ed. *The Polysaccharides*; Academic Press: New York, 1982; Vol. 1.
(22) Hineno, M. *Carbohydr. Res.* **1977**, *56*, 219.
(23) Mathlouthi, M.; Koenig, J. L. *Adv. Carbohydr. Chem. Biochem.* **1986**, *44*, 7.
(24) Mackie, W. *Carbohydr. Res.* **1971**, *20*, 413.
(25) Sakugawa, K.; Ikeda, A.; Takemura, A.; Ono, H. *J. Appl. Polym. Sci.* **2004**, *93*, 1372.
(26) Filippov, M. P.; Kohn. R. *Chem. Zvesti* **1974**, *28*, 817.
(27) Chandía, N. P.; Matsuhiro, B.; Vásquez, A. E. *Carbohydr. Polym.* **2001**, *46*, 81.
(28) Sartori, C.; Finch, D. S.; Ralph, B.; Gilding, K. *Polymer* **1997**, *38*, 42.
(29) Ryczowski, J. *Catal. Today* **2001**, *68*, 263.
(30) Knözinger, H.; Huber, S. *J. Chem. Soc., Faraday Trans.* **1998**, *94*, 2047.
(31) Buzzoni, R.; Bordiga, S.; Ricchiardi, G.; Spoto, G.; Zecchina, A. *J. Phys. Chem.* **1995**, *99*, 11937.
(32) Zecchina, A.; Spoto, G.; Bordiga, S. *Phys. Chem. Chem. Phys.* **2005**, *7*, 1627.
(33) Valentin, R.; Molvinger, K., Quignard, F.; Di Renzo, F. *Macromol. Symp.* **2005**, *222*, 93.
(34) Valentin, R.; Molvinger, K.; Quignard, F.; Brunel, D. *New J. Chem.* **2003**, *27*, 1690.
(35) Zecchina, A.; Marchese, L.; Bordiga, S.; Pazé, C.; Gianotti, E. *J. Phys. Chem. B* **1997**, *101*, 10128.
(36) Fiorilli, S.; Onida, B.; Bonelli, B.; Garrone, E. *J. Phys. Chem. B* **2005**, *109*, 16725.
(37) Chenite, A.; Chaput, C.; Combes, C.; Selmani, A. Canadian Patent 2,219,399, 2002.
(38) Martinsen, A.; Storrø, I.; Skjåk-Bræk, G. *Biotechnol. Bioeng.* **1992**, *39*, 186.
(39) Di Renzo, F.; Valentin, R.; Boissière, M.; Tourrette, A.; Sparapano, G.; Molvinger, K.; Devoisselle, J. M.; Gérardin, C.; Quignard, F. *Chem. Mater.* **2005**, *17*, 4693.
(40) Lide, D. R., Ed. *CRC Handbook of Chemistry and Physics*, 75th ed.; CRC Press: Boca Raton, FL, 1994; pp 9−78.
(41) Busca, G.; Martra, G.; Zecchina, A. *Catal. Today* **2000**, *56*, 361.
(42) Legon, A. C. *Chem. Soc. Rev.* **1993**, 153.
(43) Barnes, A. J.; Legon, A. C. *J. Mol. Struct.* **1998**, *448*, 101.
(44) Haug, A.; Smidsrød, O. *Acta Chem. Scand.* **1970**, *24*, 843.
(45) Walter, R. H.; Jacon, S. A. *Food Hydrocoll.* **1994**, *8*, 469.

BM050559X